conserve space. In either system, one can clearly see that the configuration geometry and lift control the outer nonlinear region only through the source and doublet distributions at the axis, in the manner described by Eq. (19). In particular, the degree of asymmetry of the outer flow is controlled primarily by σ. In the domain $\sigma \ll 1$, the solution to Eqs. (19–21) approaches an axisymmetric one, bearing out the area rule; but the lift and other asymmetry effects being of the orders $\sigma \equiv \alpha\lambda^{3/2}\tau^{-1/2}$ and $(\tau\lambda^3)^{1/2}$, are not all together negligible for $\lambda = 0(1) \neq 0$ [refer to Eq. (19)]. It is of interest to note from Eq. (19) that even at zero lift, there is a correction proportional to $(\tau\lambda^3)^{1/2}$ $(d/dx)(\bar{x}_j S)$, which is numerically small for most configurations but is appreciable for planforms without bilateral symmetry, such as example c in Fig. 1.[12]

Equivalence Rule and Similitude

Inspection of Eqs. (17–19) for $\sigma \leqq 0(1)$ and the corresponding system for $\sigma \gg 1$ reveals that the similarity parameters, in addition to K, are $M_\infty(\gamma + 1)^{1/2}\sigma$ and $M_\infty\{(\gamma + 1)\tau\lambda^3\}^{1/2}$. The more important features of the similitude are the equivalence rule implied by Eq. (19) and the corresponding equation for $\sigma \gg 1$. In terms of the variables x, η, ω and Φ, the nonlinear field structure as well as the far-field pattern are invariant so long as K is fixed and the equivalent source and doublet distributions, i.e.,

$$dS/dx \quad \text{and} \quad M_\infty(\gamma + 1)^{1/2}\{\sigma f_j - (\tau\lambda^3)^{1/2}(d/dx)(\bar{x}_j S)\} \qquad (20)$$

remain the same. This rule requires the same cross-sectional area distribution; the same lateral force distribution is, however, not strictly required when σ and $(\tau\lambda^3)^{1/2}$ are comparable.

Remarks

The frame work of the study outlined above may be defined, instead of Eq. (2), by $|M_\infty - 1| \ll 1$, $(\tau\lambda^3)^{1/2} \ll 1$ and $\alpha\lambda^3 \ll 1$. This may be compared with the requirements in a formulation by Cole[13] for a class of high aspect ratio wings, namely $|M_\infty - 1| \ll 1$, $\tau \ll 1$, $\tau\lambda^3 = 0(1) = \alpha\lambda^3$. Therefore, the present formulation, together with Cole's, encompasses the whole range of λ. However, like the classical slender-body theory[6–8] the present formulation is not directly applicable to rectangular planforms, the vicinity of the straight trailing edge of a flat-plate triangular wing, as well as the neighborhood of any station containing a slope discontinuity in the surface or planform. A fuller development of the theory, with supporting numerical analyses, will appear in subsequent papers. The relations of the present research to other transonic studies (flowfield computation, far-field analysis, critical-wing design, etc.) are discussed in Ref. 14.

References

[1] Whitcomb, R. T., "A Study of the Zero-lift Drag Rise Characteristics of Wing Body Combinations Near the Speed of Sound," RM-L52H08, 1952, NACA.

[2] Oswatitsch, K. and Keune, F., "Ein Äquivalenzsatz für Nichtangestellte Flügel Kleiner Spannweite in Schallnäher Strömung," *Zeitschrift für Flügwissenschaft*, Vol. 3, No. , 1954, pp. 29 46.

[3] Guderley, K. G., *The Theory of Transonic Flow*, Pergamon Press, New York, 1962.

[4] Cole, J. D. and Messiter, A. F., "Expansion Procedures and Similiarity Laws for Transonic Flow, Part. I. Slender Bodies at Zero Incidence," *Zeitschrift für Angewandte Mathematik und Physik*, Vol. 8, 1957, pp. 1–25.

[5] Ashley, H. and Landahl, M., *Aerodynamics of Wings and Bodies*, Addison-Wesley, Reading, Mass., 1965.

[6] Jones, R. T., "Properties of Low-Aspect Ratio Pointed Wings at Speeds Below and Above the Speed of Sound," Rept. 835, 1946, NACA.

[7] Ward, G. N., "Supersonic Flow Past Slender Pointed Bodies," *Quarterly Journal Mechanics and Applied Mathematics*, Vol. 2, Pat. 1, 1949, pp. 75–97.

[8] Adams, M. C. and Sears, W. R., "Slender-Body Theory—Review and Extensions," *Journal of the Aeronautical Sciences*, Vol. 20, No. 2, 1953, pp. 85–98.

[9] Spreiter, J. R. and Stahara, S. S., "Aerodynamics of Slender Bodies and Wing-Body Combinations at $M_\infty = 1$," *AIAA Journal*, Vol. 9, No. 9, Sept. 1971, pp. 1784–1791.

[10] Murman, E. M. and Cole, J. D., "Calculation of Plane Steady Transonic Flows," *AIAA Journal*, Vol. 9, No. 1, Jan. 1971, pp. 114–121.

[11] Krupp, J. A. and Murman, E. M., "The Numerical Calculation of Steady Transonic Flows Past Thin Lifting Airfoils and Slender Bodies," AIAA Paper 71-566, Palo Alto, Calif., 1971.

[12] Jones, R. T., "Reduction of Wave Drag by Antisymmetric Arrangement of Wings and Bodies," *AIAA Journal*, Vol. 10, No. 2, Feb. 1972, pp. 171-176.

[13] Cole, J. D., "Twenty Years of Transonic Flows," Document D1-82-0878, July 1969, Boeing Scientific Research Lab., Seattle, Wash.

[14] Cheng, H. K. and Hafez, M., "On Three Dimensional Structure of Transonic Flows," Rept. USCAE 121, July 1972, Univ. Southern Calif., Aerospace Engineering Dept., Los Angeles, Calif.

Cooled Supersonic Turbulent Boundary Layer Separated by a Forward Facing Step

FRANK W. SPAID*
University of California, Los Angeles, Calif.

Nomenclature

C_f = skin-friction coefficient
C_p = pressure coefficient
$\bar{C}_p$ = free interaction parameter, $\bar{C}_p = C_{fo}{}^{1/2}(M_0^2 - 1)^{-1/4}$
h = step height
M = Mach number
p = pressure
Re = Reynolds number
T = temperature
x = coordinate axis aligned with flow direction, with origin at the step
Δx = x distance measured from the beginning of the interaction
δ = boundary-layer thickness

Subscripts
o = undisturbed flow just upstream of the interaction
p = conditions at the plateau, or first peak in the static pressure distribution
r = conditions corresponding to recovery temperature
w = conditions at the wall

THE objective of the present study was to investigate the effect of wall cooling on separation of a turbulent boundary layer by a forward-facing step in supersonic flow.

Experimental Apparatus and Technique

Experiments were conducted on the nozzle wall of the 3 × 3 in. supersonic wind tunnel of the UCLA Aerodynamics Laboratory, at a nomical Mach number of 2.9. The nozzle block on that side was water-cooled over its entire length. A water-cooled brass model which included an adjustable step formed one of the test section walls.

Model static pressures were measured at 30 locations with the aid of two Scanivalves and a 0–5 psid transducer. Model and nozzle block temperatures were sensed at 13 locations by iron-constantan thermocouples.

Pitot pressure and stagnation temperature surveys of the undisturbed boundary layer on the test section wall were conducted at several locations, for each test condition. Displacement thicknesses were consistent with the assumption that transition

Received March 3, 1972; revision received April 13, 1972. This work was supported by the School of Engineering and Applied Science, and by the Campus Computing Network, University of California, Los Angeles.

Index category: Jets, Wakes, and Viscid-Inviscid Flow Interactions.

* Assistant Professor, School of Engineering and Applied Science. Member AIAA.

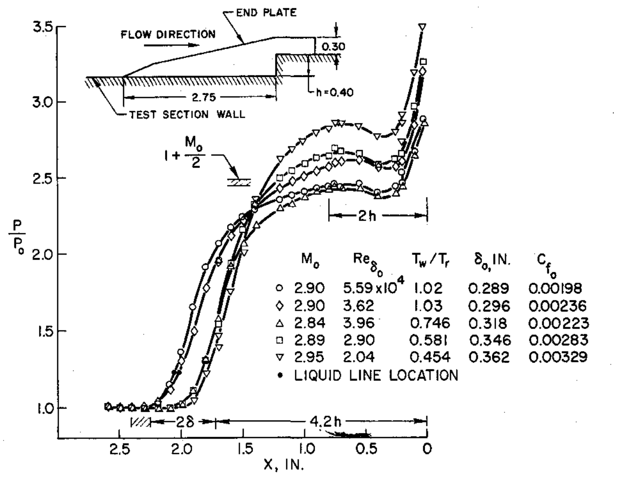

Fig. 1 Static pressure distributions upstream of the 0.40 in. step.

occurred near the nozzle throat. Skin-friction measurements were made with Preston tubes, using the calibration of Keener and Hopkins.[1] Boundary-layer profiles were transformed by the method of Baronti and Libby,[2] and all transformed profiles agree quite well with the incompressible law of the wall. Stagnation temperature profiles obtained with wall cooling showed lower values of stagnation temperature than those corresponding to the Crocco relation.

The experiments were conducted with the same apparatus and at the same test section conditions described in Refs. 3 and 4, which contain additional information concerning the model, instrumentation, and boundary-layer surveys.

Experiments were conducted with an 0.40-in. step with the model sealed against the tunnel side walls, without end plates and with two end plate designs. The end plates were made from 0.010 in. brass sheet, spaced 2.00 in. in the spanwise direction, aligned with the flow direction, and sealed to the model with the flow direction, and sealed to the model with silicone rubber. Two-dimensionality of the flow was evaluated from observation of oil-flow patterns, and by spanwise variation in static pressure at $x = 0.2$ and 1.7 in. Both methods indicated that flowfields obtained with the end plate design of Fig. 1 were reasonably two-dimensional. Observations made with a smaller set of end plates and without end plates showed successively greater departures from two-dimensionality. Axial distributions of static pressure along the test section centerline were quite insensitive to these variations. All data presented here were obtained with the end plate design of Fig. 1.

Discussion of Results

Static pressure data obtained with the 0.40 in. step are presented in Fig. 1. Spanwise variation in static pressure distribution is indicated for two cases, which are typical of all test conditions. The review of data by Zukoski,[5] which included adiabatic flow over a wide range of Mach number and Reynolds number, showed that the first peak in the pressure distribution occurred at a distance of approximately $2h$ upstream of the step, that the first peak or plateau pressure could be correlated by the expression $p_p/p_o = 1 + M_o/2$, that the distance from the step to the separation point (located approximately at $(P - P_0)/(P_p - P_0) = 0.73$) was approximately $4.2h$, and that the maximum extent of the interaction region upstream of the step was $4.2h + 2\delta$. Adiabatic data obtained at the maximum Reynolds number of this investigation agree quite well with these correlations. Data for turbulent boundary layers at low Reynolds number tend to show an increase in P_p/P_0 with decreasing Reynolds number, and the present adiabatic data also show the same tendency. A series of data is presented in which T_w/T_r and Re_{δ_o} were both varied. These data show an increase in P_p/P_0 and a decrease in the upstream extent of the interaction, with decreasing T_w/T_r and Re_{δ_0}. The location of the first peak in the static pressure distribution did not change appreciably.

Dots on the static pressure plots mark the liquid line locations, which could be observed only under adiabatic wall conditions. A comparison between liquid line locations and results of a dust deposit technique has shown good agreement.[3,4] The values of P/P_0 at the liquid line location are essentially the same as those obtained from earlier compression-corner experiments.[3,4] The location of separation as determined from pitot-pressure or hot-wire data is usually somewhat closer to the step.[5,6]

The trends shown in Fig. 1 are substantiated by data obtained at intermediate Reynolds numbers with the 0.40 in. step, and with a comparable set of data taken with a 0.31 in. step.

Plateau pressure coefficient data, normalized by a scale factor obtained from the free interaction theory of Chapman et al.,[7] are presented in Fig. 2. These data support the interpretation that the variation in C_{p_p} with heat transfer or Reynolds number is associated with the corresponding variation in C_{f_0}, in contrast to the Reynolds number independence of C_{p_p} which is observed for adiabatic flow at higher Reynolds numbers.[5]

A comparison between data from these experiments and a correlation suggested by Zukoski is made in Fig. 3. Data are presented for the region between the beginning of the interaction and the first peak in the pressure distribution. The solid lines represent the range of variation of the adiabatic data presented in Ref. 5, which correspond to $h/\delta_0 > 1$ and $2 \leq M < 6$. Agreement between the present data and the correlation is generally good for $(P - P_0)/(P_p - P_0) < 0.5$, including the value of the maximum pressure gradient. Downstream of this point the data reviewed in Ref. 5 showed a tendency to scale with h, rather than δ_0, so that the average pressure gradient in this region tended to decrease with increasing h/δ_0. This trend is approximately consistent with the present data for $T_w/T_r < 1$ shown in the upper part of Fig. 3, where the pressure rise to the first peak becomes more abrupt as the over-all length of the interaction decreases.

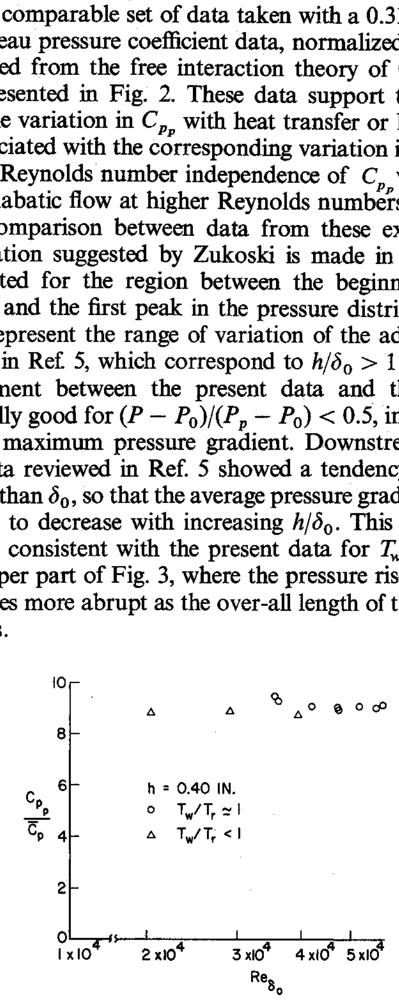

Fig. 2 Plateau pressure coefficients normalized by free interaction parameter.

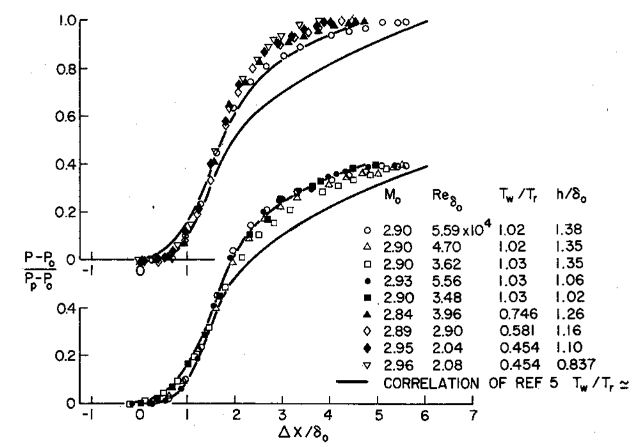

Fig. 3 Static pressure distributions from the present experiments compared with the correlation of Ref. 5.

Conclusions

Results of the present experiments show increasing plateau pressure and decreasing length of the interaction region with decreasing Reynolds number and decreasing wall-to-recovery temperature ratio. Values of plateau pressure coefficient were proportional to the square root of the skin-friction coefficient of the undisturbed boundary layer, a scaling law derived from Chapman's formulation of free interaction, and maximum static pressure gradients were found to agree reasonably well with Zukoski's correlation of adiabatic data.

References

[1] Keener, E. R. and Hopkins, E. J., "Use of Preston Tubes for Measuring Hypersonic Turbulent Skin Friction," TN D-5544, Nov. 1969, NASA.

[2] Baronti, P. O. and Libby, P. A., "Velocity Profiles in Turbulent Compressible Boundary Layers," *AIAA Journal*, Vol. 4, No. 2, Feb. 1966, pp. 193–202.

[3] Spaid, F. W. and Frishett, J. C., "Incipient Separation of a Supersonic, Turbulent Boundary Layer, Including Effects of Heat Transfer," AIAA Paper 72-114, San Diego, Calif., 1972.

[4] Frishett, J. C., "Incipient Separation of a Supersonic, Turbulent Boundary Layer, Including Effects of Heat Transfer," Ph. D. thesis, Sept. 1971, Univ. of California, Los Angeles.

[5] Zukoski, E. E., "Turbulent Boundary-Layer Separation in Front of a Forward-Facing Step," *AIAA Journal*, Vol. 5, No. 10, Oct. 1967, pp. 1746–1753.

[6] Behrens, W., "Separation of a Supersonic Turbulent Boundary Layer by a Forward Facing Step," AIAA Paper 71-127, New York, 1971.

[7] Chapman, D. R., Kuehn, D. M., and Larson, H. K., "Investigation of Separated Flows in Supersonic and Subsonic Streams with Emphasis on the Effect of Transition," Rept. 1356, 1958, NACA.

Direct Measurement of the Velocity Gradient in a Fluid Flow

ROBERT H. KIRCHHOFF* AND EUGENE K. VOCI†

University of Massachusetts, Amherst, Mass.

Introduction

THE usual technique of constructing the velocity gradient in a fluid flow is to measure the velocity profile and then numercally or graphically differentiate the data. This technique is inherently inaccurate because it is an averaging technique. Points of inflection and large gradients in the velocity profile are either inaccurately measured or not detected.

In this research, a fundamental extension of the hot-wire technique was used to measure directly the gradient of the mean velocity profile. Basically, the method requires the use of a vibrating hot-wire anemometer. It will be shown that the oscillatory anemometer response is proportional to the velocity gradient in the flow. Detection of the oscillatory signal of the hot-wire at the frequency of forced oscillation with a Lock-In Amplifier (LIA) gives the direct measurement of the velocity gradient.

The technique has direct application to the diagnosis of stratified flows, the fluid mechanics of the air-sea interface, and the phenomeonological description of turbulence.

Received March 3, 1972; revision received April 12, 1972. This research was supported in part by the National Science Foundation under Grant NSF GK 30481.

Index category: Research Facilities and Instrumentation.

* Assistant Professor, Department of Mechanical and Aerospace Engineering. Member AIAA.

† Graduate Assistant; presently Staff Engineer, Stone and Webster, Boston, Mass.

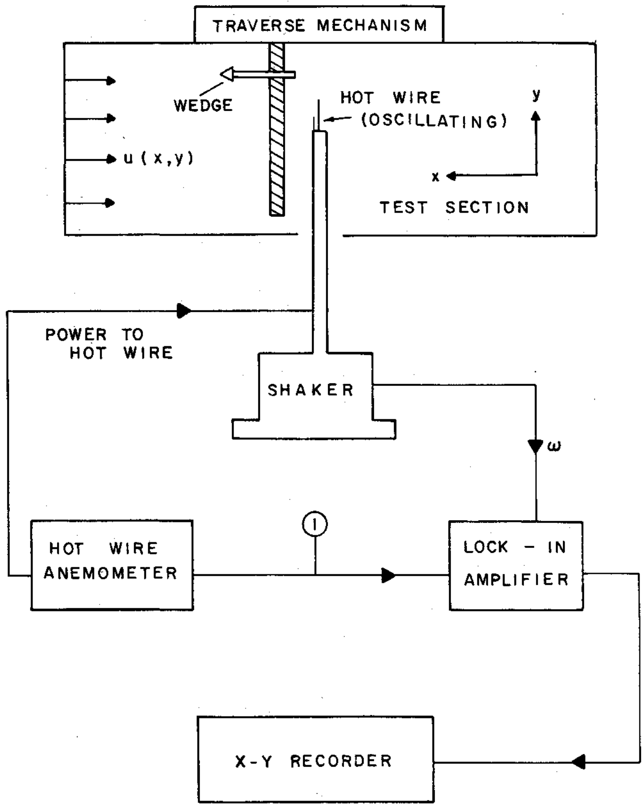

Fig. 1 Experimental schematic.

Theory

Figure 1 is a schematic of a hot wire probe oscillating in a fluid flow of mean velocity $u(x, y)$. The probe is constrained to oscillate in the y-z plane perpendicular to the velocity $u(x, y)$. The wire performs simple harmonic motion according to the relation

$$y(t) = y_0 + R \sin \omega t \tag{1}$$

where R is the amplitude of the oscillation at a fixed point x_0, and ω is the radian frequency of forced oscillation. The velocity V as seen by the probe may be written as

$$V = [u(x,y)^2 + (\omega R)^2 \cos^2 \omega t]^{1/2} \tag{2}$$

Suppressing the argument x, the velocity $u^2(y)$ may be expanded in a Taylor series about y_0 and combined with Eq. (1) and (2) to form the following relation for the velocity V as seen by the probe

$$V^2(t) = u^2 + (R^2/2)(uu'' + u'^2 + \omega^2) + \sin \omega t \{2uu'R + (R^3/4)(uu''' + 3u'u'')\} + \cos 2\omega t \{(\omega R)^2/2 - R^2u'^2/2 - R^2uu''/2\} + \sin 3\omega t \{-R^3/12(uu''' + 3u'u'')\} + \ldots \tag{3}$$

Let δ be the scale length of the gradient of u in the y direction. Define a dimensionless distance $y^* = y/\delta$ and a dimensionless velocity $u^* = u/U_\infty$. Equation (3) may then be written as

$$V^2(t) = U_\infty{}^2 \{u^*2 + \tfrac{1}{2}(R/\delta)^2 (u^*u''^* + u'^{*2} + \omega^2) + [2u^*u'^*R/\delta + (R/\delta)^3 (u^*u'''^*/4 - \tfrac{3}{4}u'^*u''^*)] \sin \omega t + [\omega^2/2(R/\delta)^2 - (R/\delta)^2 u'^{*2}/2 - (R/\delta)^2 u^*u''^*/2] \cos 2\omega t + [-(R/\delta)^3 (u^*u'''^*/12 + u'^*u''^*/4)] \sin 3\omega t + \ldots\} \tag{4}$$

If R/δ can be made $<< 1$ and consideration is given to the coefficient of $\sin \omega t$ then Eq. (3) may be written approximately as

$$V^2(t) \simeq 2uu'R \sin \omega t \tag{5}$$

Similarly if it is desired to consider terms at frequency 2ω, then Eq. (3) may be written approximately as

$$V^2(t) = (R^2/2)[\omega^2 - u'^2 - uu''] \cos 2\omega t \tag{6}$$

If the oscillatory amplitude of $V^2(t)$ could be measured at the forcing frequency, ω or 2ω, and a known amplitude of oscillation,